Mechanism of α-lipoic acid action on copper metabolism studied in cell culture and *Drosophila* models

Master's thesis

Gertrud Henna Sildnik

Supervisors:

Sigrid Kirss, MSc

Department of Chemistry and Biotechnology

Professor Peep Palumaa

Department of Chemistry and Biotechnology

Study program: Applied Chemistry and Biotechnology

Tallinn 2022

α-lipoehappe toimemehhanism vase metabolismile rakukultuuri ja äädikakärbse mudelites

Magistritöö

Gertrud Henna Sildnik

Juhendajad:

Sigrid Kirss, MSc

Keemia ja biotehnoloogia instituut

Professor Peep Palumaa

Keemia ja biotehnoloogia instituut

Õppekava: Rakenduskeemia ja biotehnoloogia

Tallinn 2022

Autorideklaratsioon

Kinnitan, et olen koostanud antud lõputöö iseseisvalt ning seda ei ole kellegi teise poolt varem kaitsmisele esitatud. Kõik töö koostamisel kasutatud teiste autorite tööd, olulised seisukohad, kirjandusallikatest ja mujalt pärinevad andmed on töös viidatud.

Autor: Gertrud Henna Sildnik

[allkiri ja kuupäev]

Töö vastab magistritööle esitatavatele nõuetele.

Juhendaja: Peep Palumaa, Sigrid Kirss

[allkiri ja kuupäev]

Töö on lubatud kaitsmisele.

Kaitsmiskomisjoni esimees:

[allkiri ja kuupäev]

Table of Contents

Abbreviations

Aβ	Amyloid-beta
ABD-F	4-(aminosulfonyl)-7-fluoro-2,1,3-benzoxadiazole
Acetone EtOAc	Acetone ethyl acetate
ACN	Acetonitrile
AD	Alzheimer's disease
APP	Amyloid precursor protein
BACE1	β-site APP cleaving enzyme 1
BBB	Blood-brain barrier
BDNF	Brain-derived neurotrophic factor
COX	Cytochrome oxidase
CQ	Clioquinol
CSF	Cerebrospinal fluid
DHLA	Dihydrolipoic acid
DMEM	Dulbecco's Modified Eagle Medium
FBS	Fetal bovine serum
FDA	Food and Drug Administration
HPLC	High-performance liquid chromatography
ICP-MS	Inductively coupled plasma mass spectrometry
LA	α-lipoic acid
NDMA	N-methyl-D-aspartate
PBS	Phosphate-buffered saline
PBT-2	5,7-dichloro-2-[(dimethylamino)methyl]quinolin-8-ol

PEST	Penicillin-streptomycin
PSEN1	Presenilin 1
PSEN2	Presenilin 2
RA	Retinoic acid
ROS	Reactive oxygen species
SEM	Scanning electron microscopy
SOD1	Superoxide dismutase 1
TCEP	Tris(2-carboxyethyl)phosphine
TFA	Trifluoroacetic acid
UAS	Upstream activation sequence
UHPLC	Ultra-high-performance liquid chromatography

Introduction

Alzheimer's disease (AD) is a progressive neurodegenerative disorder and the leading cause of dementia. AD is characterized by extracellular amyloid plaques consisting of amyloid-β (Aβ) peptides, and intracellular neurofibrillary tangles, composed of hyperphosphorylated tau protein. There are approximately 55 million people in the world affected by this disease.

The etiology of AD is yet unknown, although many hypotheses have been proposed. The most well-known is the amyloid cascade hypothesis, which suggests that the accumulation of Aβ peptides into plaques is the causative factor of AD, after which follows the formation of intracellular neurofibrillary tangles and, eventually, neurodegeneration. Among the other hypotheses are the tau and metal hypotheses.

Due to the higher metabolic rate of the brain, the concentrations of biometals are elevated. However, it has been shown that in the case of AD, the homeostasis of biometals is altered. During the aggregation of Aβ peptides, interactions with mainly Cu(II) but also Fe(III) and Zn(II) ions occur. Importantly, it has been shown that the concentration of copper ions is high in amyloid plaques, leaving the cells in deficiency.

Based on the copper dyshomeostasis hypothesis, we propose the use of α-lipoic acid (LA) as a copper redistributing agent. Our group has shown that LA binds Cu(I) ions with high affinity and translocates copper ions from the extracellular into the intracellular environment. Our recently published article showed that LA improves the locomotor activity of the transgenic AD fly model. However, the mechanism of LA action on copper metabolism has not been investigated.

In the current study, ICP-MS and UHPLC were used to investigate the kinetics of copper transport by LA and the cellular accumulation of LA in differentiated SH-SY5Y neuroblastoma cell line. The effect of LA on copper-induced neurodegeneration was also investigated in the APP/Bace1 AD *Drosophila melanogaster* model.

This study showed that LA has a relatively slow action on copper metabolism, however, the accumulation of LA in the cells occurs faster. LA also has an *in vivo* protective effect on copper-induced neurodegeneration in the AD *Drosophila* model with eye-specific human APP and Bace1 overexpression.

1 Review of literature

1.1 Alzheimer's disease

Alzheimer's disease (AD) is a progressive neurodegenerative disease and the leading cause of dementia, which was first described by Alois Alzheimer in 1906 [1]. According to the World Health Organization, dementia is currently the seventh leading cause of death. There are over 55 million people in the world affected by dementia, with the number increasing yearly by 10 million [2].

AD is a multifactorial disease that results in extensive loss of neurons leading to cognitive decline. AD's pathology is characterized by extracellular amyloid plaques composed of amyloid-β (Aβ) peptides, and intracellular neurofibrillary tangles, consisting of hyperphosphorylated tau protein. These pathological hallmarks are primarily found in brain areas associated with cognition, e.g., the hippocampus and neocortex [3]. With the disease progressing, these hallmarks can also be found in other brain areas [4].

Amyloid plaques are formed through the oligomerization and aggregation of Aβ peptides, which are cleavage products of amyloid precursor protein (APP). APP is a transmembrane protein that is highly expressed in the brain and is mainly concentrated in nerve terminals [5]. Its functions are not entirely understood, however, it is known that APP likely participates in synaptic formation and neurite outgrowth [6]. Normally, APP is cleaved by α- and γ-secretase in the non-amyloidogenic pathway, in which pathogenic Aβ peptides are not produced. In the diseased state, APP is mainly processed in the amyloidogenic pathway sequentially by the β-secretase (β-site APP cleaving enzyme 1, BACE1) and γ-secretase, which results in the formation of Aβ peptides [7]. The length of these peptides may vary from 38 to 43 as there are various cleavage sites for γ-secretase [8]. In the amyloid plaques, Aβ is mainly found in the forms of Aβ40 and Aβ42, with the latter being more hydrophobic and, thus, more prone to aggregation [9].

While over 90% of AD cases are sporadic, mutations in amyloid precursor protein (*APP*), presenilin 1 (*PSEN1*), and presenilin 2 (*PSEN2*) genes are related to a rare familial form of the disease [10]. Approximately 80% of the mutations associated with AD have been found in the *PSEN1* gene [11], coding presenilin 1, which is a subunit of the APP cleaving γ-secretase complex [12]. The mutations in *APP* are located in or near the Aβ sequence, while mutations in the *PSEN1* and *PSEN2* are distributed throughout the protein-coding regions [13]. These mutations are mainly associated with modification of enzymatic function and lead to AD by altered APP processing and elevated Aβ42/40 ratio [14].

The most significant risk factor for AD is age, with the disease affecting primarily people over the age of 65. However, familial AD has early-onset pathogenesis, in which the disease can impact patients already in their thirties or forties [15]. Moreover, women are more subjected to developing AD compared to men. It has also been found that the *ApoE* ε4 allele is related to a higher risk for

sporadic AD compared to other alleles of this gene [16]. Other risk factors include type 2 diabetes, obesity, cerebrovascular diseases, hypertension, and dyslipidemia [17].

Despite decades of research, the etiology of AD remains still unknown. However, there are numerous hypotheses, of which the most extensively researched is the amyloid cascade hypothesis [18]. It proposes that the accumulation of Aβ peptides into plaques is the causative factor of AD pathology, after which follows the formation of neurofibrillary tangles. These processes lead to activated immune reactions and neurodegeneration. Other hypotheses include the tau, oxidative stress, and metal hypothesis [19].

1.2 The role of metal ions in neurodegenerative diseases

Higher levels of biometal ions are essential in the brain for synaptic transmission and other neurological functions [20]. Compared to other organs, the brain has higher oxygen consumption and lower antioxidant levels and is, therefore, more susceptible to oxidative stress [21]. Hence, the homeostasis and transport of metal ions must be strictly regulated.

Iron is the most abundant trace metal in humans, participating in cell division, oxygen transport, and mitochondrial function. In the brain, iron participates in myelination and neurotransmitter synthesis and signaling [22]. As a redox-active metal, it also plays an important role in oxidative stress. It participates in Fenton and Haber-Weiss reactions, in which reactive oxygen species (ROS) are produced. Hydroxyl radicals are the most reactive ROS, which can target most biomolecules by disrupting their functions, leading to oxidative stress and causing cell death [23]. During aging, iron accumulates in the brain, which may contribute to neurodegenerative diseases [24-27].

Zinc is the second most abundant trace metal, necessary for numerous processes, e.g., DNA replication and protein synthesis [28]. More than 300 enzymes require zinc for their functioning [29]. In the brain, 80% of zinc is bound to metalloproteins, and the remaining unbound zinc is concentrated in the presynaptic vesicles of glutamatergic neurons [30]. Zn has been implicated in playing a pivotal role in various neurodegenerative disorders, such as AD, Parkinson's disease, and multiple sclerosis [31].

In the case of AD, the aggregation of Aβ involves interactions with extracellular Cu, Zn, and Fe ions, therefore, depriving cells of necessary metals required for normal cellular functioning [32]. It has been shown that Cu, Fe, and Zn ions are found in amyloid plaques in two- to five-fold higher concentrations than normal [33]. Aβ catalyzes the reduction of redox-active Cu(II) and Fe(III) ions, which leads to the generation of ROS and may contribute to oxidative stress [34].

1.2.1 The role of copper in Alzheimer's disease

Copper is the third most abundant trace metal in humans [35], which is vital for numerous biological processes as a cofactor and a structural component of proteins. It participates in energy metabolism, antioxidative defense, neurotransmitter, and neuropeptide synthesis [36].

The primary copper transporters are Ctr1, ATP7A, and ATP7B [37], whereas the uptake is mediated by Ctr1 and the efflux by ATP7A or ATP7B. Copper is transported to the brain from the periphery through the blood-brain barrier (BBB) and is released into the brain parenchyma, where it is utilized. Excess copper is then released into the cerebrospinal fluid (CSF), where it can be taken up for storage or is released into the blood [36].

The content and distribution of copper have been reported to change with aging and in the case of neurodegenerative diseases [27, 38, 39]. Copper levels are shown to be lower in the AD brain tissue, especially in the hippocampus and amygdala regions. In contrast, the content of labile copper is higher in the extracellular environment [40, 41].

The altered metabolism of copper in the AD brain has been linked to the dysfunction of several necessary enzymes, such as Cu/Zn-superoxide dismutase (SOD1) and cytochrome c oxidase (COX), which are crucial for maintaining metabolic homeostasis [42]. The normalization of copper metabolism may restore the normal functioning of these enzymes [43].

Cu(II) ions bind to Aβ with picomolar affinity and induce the oligomerization of Aβ peptides [44, 45]. When copper is bound to Aβ, it cycles between the reduced and oxidized states. Through the reduction of Cu(II) to Cu(I), hydrogen peroxide can be produced, which may subsequently lead to the production of highly reactive hydroxyl radicals through the Fenton-type reactions [46].

In vitro experiments have shown that the removal of Cu(II) ions from Aβ inhibits its aggregation process and decreases the production of H_2O_2 [47].

1.3 Therapies

In 2021, there were 126 agents in clinical trials for AD, with most of the agents targeted for amyloid reduction. There was a modest increase of agents in the clinical trials compared to 2020, likely due to the increasing diversity of targets and therapeutic approaches [48].

The Food and Drug Agency (FDA) recently approved amyloid targeting monoclonal antibody Aducanumab, being currently the only disease-modifying drug available for AD. However, the data regarding its efficacy is contradictory as there is no clear relationship between the reduction of amyloid plaques and cognitive improvement [49].

Also, four symptomatic drugs for AD are available, which include three cholinesterase inhibitors (donepezil, galantamine, and rivastigmine) and one N-methyl D-aspartate (NMDA) receptor antagonist (memantine) [50].

Metal chelation therapy has been proposed as a possible treatment for AD. However, as metal ions are crucial for the brain's normal functioning, finding a selective and specific chelating agent is a challenge. Clioquinol (5-chloro-7-iodo-8-hydroxyquinoline, CQ) has been investigated as a metal chelator to redistribute metal ions from metal-Aβ complexes to avoid cellular metal deficiency. It was shown to remove Cu(II) and Zn(II) ions from precipitated Aβ peptides in post-mortem AD brain [51] and inhibited the formation of amyloid aggregates in transgenic APP2576 mice [52]. However, the trials with CQ were terminated as it was found to be neurotoxic [53]. A derivative of CQ, 5,7-dichloro-2-((dimethylamino)methyl)quinolin-8-ol (PBT-2), was also investigated as a possible candidate as it showed greater efficacy in reducing Aβ deposition in transgenic mice [54]. However, it did not exhibit significant effects in clinical trials [53].

1.3.1 α-lipoic acid as a therapeutic agent in AD

α-lipoic acid (LA), also known as thioctic acid, is a naturally occurring cofactor of different multienzyme complexes in prokaryotic and eukaryotic cells [55], such as pyruvate dehydrogenase, α-ketoglutarate dehydrogenase, branch-chained α-ketoacid dehydrogenase and 2-oxoadipate dehydrogenase [56]. LA is produced in small amounts in the mitochondrion from octanoic acid but is mainly consumed through exogenous sources as it is found in various vegetables and meat [57].

LA has two enantiomeric forms: R- and S-LA. Whereas LA is found in nature as an R enantiomer, supplements available in pharmacies are composed of a racemic mixture of R and S enantiomers [58].

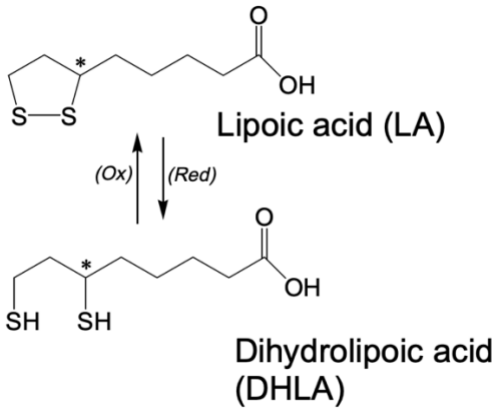

Figure 1. Chemical structure of α-lipoic acid and its reduced form dihydrolipoic acid [55].

In the cell, LA is reduced to dihydrolipoic acid (DHLA) (Figure 1) [59], which has more substantial antioxidant properties compared to LA. However, both are efficient scavengers of ROS, such as

hydroxyl radicals [60] and can cross the BBB [61]. DHLA has been shown to increase the synthesis of acetylcholine esterase and glutathione [62] and chelate redox-active transition metals [63].

LA has been suggested in the treatment of diabetic peripheral neuropathy and has been proposed in the treatment of AD and other dementias for its neuroprotective and metal-binding properties [64].

A recently published article demonstrated that LA improved memory impairment in rat models of AD-type dementia [65]. The supplementation of LA has also been evaluated on aged Tg2576 mice overexpressing APP, where LA was shown to improve learning and memory, however, no effect on amyloid plaque deposition was observed [66].

It has been shown earlier by our group that DHLA binds Cu(I)-ions intracellularly with an affinity of K_d=8.05 x 10^{-17} M [67] and improves the locomotor activity of *Drosophila* AD models [68]. We have also shown that LA affects copper metabolism by translocating it from the extracellular environment into the intracellular, however, the exact mechanism of LA action has not yet been investigated.

2 Aims of the study

The current study was directed towards elucidating the mechanism of α-lipoic acid action on copper metabolism. In particular:

1) to study the kinetics of LA-promoted copper transport in differentiated SH-SY5Y cell culture by using ICP-MS;
2) to study the kinetics of LA cellular accumulation in differentiated SH-SY5Y cell culture by using UHPLC;
3) to investigate the effect of LA on copper-induced neurodegeneration in APP/Bace1 AD *Drosophila* models.

3 Materials and methods

3.1 Theoretical description

3.1.1 SH-SY5Y cell line

The SH-SY5Y cell line is a third subclone of the SK-N-SH line originating from human neuroblastoma. SH-SY5Y cultures are heterogenous, comprising neuroblast- and epithelial-like cells [69]. Undifferentiated SH-SY5Y cells form clumps where cells grow on top of one another as they continuously proliferate [70].

The SH-SY5Y cell line is widely used for its ability to differentiate into homogenous neuron-like phenotype. Differentiation of SH-SY5Y cells reduces proliferation and induces the expression of many typical neuronal markers. Several agents are used for differentiation, however, retinoic acid (RA) and brain-derived neurotrophic factor (BDNF) in a serum-free medium are mainly used. Treatment with RA induces the formation of neurites and makes the cells receptive to BDNF [71, 72].

3.1.2 *Drosophila melanogaster* as a model organism

Fruit flies are one of the most widely used model organisms to research human disorders, including neurodegenerative diseases. They are also one of the first organisms with a fully sequenced genome with approximately 14 000 protein-coding genes [73]. Fruit flies have four chromosomes (X/Y, II, III, and IV), with most of the genes located on chromosomes X, II, and III [74].

One of the essential advantages of using fruit flies is that approximately 75% of the genes involved in human diseases have orthologs in *Drosophila* [74]. Another important advantage of fruit fly model organisms is that they have balancer chromosomes, which allow the maintenance of mutations or transgenes [75].

Fruit flies have a short generation time (~10 days) and lifespan (~60-80 days), which make them even more ideal in the studies of age-related diseases [76].

The life cycle of *Drosophila* is 9-11 days at 25 °C. It takes approximately 24 h for an egg to undergo embryogenesis and hatch as a first instar larva. After another 24 h, the first instar larva molts larger into a second instar larva. Then, the larva undergoes a molt into a third instar larva, which digs into the food. After approximately 2 days, the larva crawls out of the food, climbs upwards onto the vial's walls, and develops into a pupa. During the next 4-6 days, the pupa transforms into an adult fly when it undergoes the eclosion from the pupal case (Figure 2) [77].

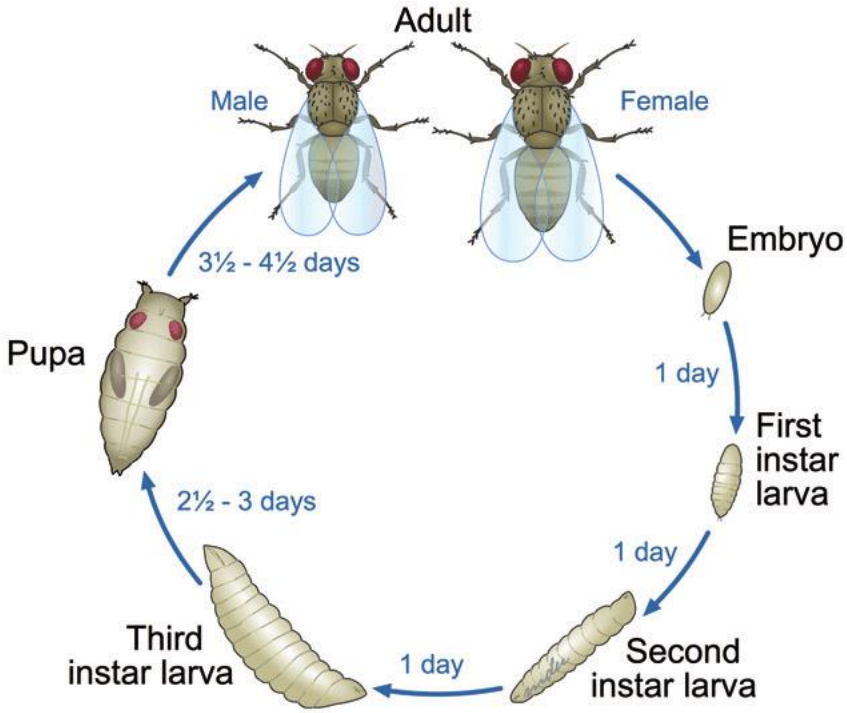

Figure 2. Fruit flies have four stages in their development: egg, larva, pupa, and adult. The life cycle of *Drosophila melanogaster* is approximately 10 days at 25 °C [78].

Female adults should be collected right after eclosion as they can mate about 12 h after emerging from the pupal case. A single female fly can lay hundreds of eggs after mating [77].

UAS-Gal4 expression system

The UAS-Gal4 expression system was first introduced by Brand and Perrimon in 1993 and is widely used for expressing transgenes in fruit flies [79]. The system comprises two components used in separate fly lines. The driver line contains yeast transcription factor Gal4, which is used to control the expression of a target gene. Gal4 is inserted downstream of a promoter element, which drives the expression of a gene in a tissue- or cell-specific manner. The responder line contains Gal4-binding upstream-activating sequence (UAS) placed upstream of a target gene. When driver and responder lines are crossed, Gal4 binds to the UAS element, and the transgene expression is activated in their progenies (Figure 3) [80].

In the current study, UAS-APP695-N-myc, UAS-BACE1/TM6B (Vitruvian; Bloomington Drosophila Stock Center (BDSC) #33797) overexpressing human APP and BACE1, and *ninaE*^{GMR}*-Gal4* (BDSC, #1104) were used for *Drosophila* experiments.

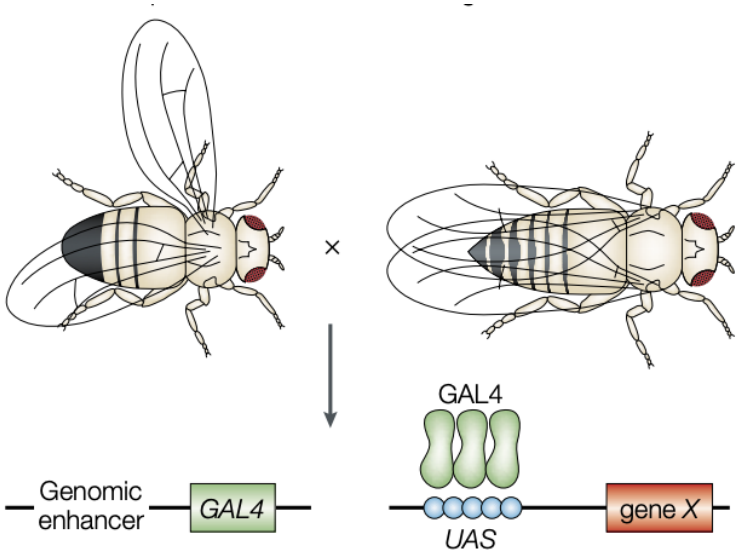

Figure 3. The UAS-Gal4 expression system is widely used in *Drosophila* for targeted gene expression. For this system, a yeast transcriptional factor Gal4 is paired with a tissue-specific enhancer in one fly line, and the transgene is paired with the UAS element in the other fly line. When crossing these two fly lines, Gal4 binds to the UAS element and activates the gene expression [81].

3.1.3 Inductively Coupled Plasma Mass Spectrometry

Inductively coupled plasma mass spectrometry (ICP-MS) is an analytical method for measuring the concentrations of metals in liquid samples. ICP-MS consists of six compartments: sample introduction, inductively coupled plasma, interface, ion optics, mass analyzer, and detector.

Sample preparation for this method is rather simple as biological samples are processed mainly using hydrochloric acid or nitric acid and diluted with deionized water. ICP-MS is used to analyze liquids; therefore, thermal digestion using strong acids or alkali might be required for some sample types, e.g., tissues.

When liquid samples are introduced to the instrument, they are first aerosolized by a nebulizer, which turns the liquid into aerosols. After nebulizing, the sample enters the spray chamber, which filters out aerosol droplets before entering the plasma, as the plasma is inefficient at dissociating large aerosol droplets. ICP uses an argon or helium plasma, which completely atomizes most molecules in the sample, reaching temperatures of 9000 °C.

The aerosol droplets exiting the spray chamber are reaching into the plasma along with the stream of argon gas. After reaching the plasma, the sample is desolvated, vaporized, atomized, and ionized. The ions formed in the plasma are transported through the interface and ion optics into a quadrupole mass analyser, where ions are separated based on their mass-charge ratio, and the detector measures the ions obtained from the samples.

The most significant advantages of this technique are low detection limits and the ability to detect multiple elements simultaneously in a single analysis [82, 83].

3.1.4 Ultra-High-Performance Liquid Chromatography

Ultra-high-performance liquid chromatography (UHPLC) is one of the most powerful and widely used chromatographic separation techniques to analyze and separate components from complex mixtures. UHPLC operates at a higher pressure and offers increased resolution and reduced analysis times compared to a regular HPLC. Also, the columns of UHPLC consist of smaller particles compared to HPLC [84].

Various column types are used in the HPLC with different adsorbent particle sizes and pore diameters, phase types, and column lengths. The adsorbents are mostly porous particles, which in reversed-phase HPLC are hydrophobic. The size of these particles affects the narrowness of the obtained peaks. Particles with smaller diameters typically produce sharp peaks with better resolution [85]. The most commonly used columns in reversed-phase HPLC are the alkyl-bonded C_{18} columns [86], which are usually applied for the separation of smaller molecules (<5000 Da) [85].

As a mobile phase solvent, acetonitrile (ACN) is most commonly used with water as it is volatile and has a low viscosity. Acetonitrile (ACN) is usually supplemented with trifluoroacetic acid (TFA) as an acidic modifier for ion-pairing, which enhances the separation [84].

3.2 Experimental procedures

3.2.1 Neuroblastoma SH-SY5Y cell cultivation and differentiation protocol

Human neuroblastoma SH-SY5Y cells were grown in Dulbecco's Modified Eagle Medium (DMEM) (Gibco) supplemented with 10% fetal bovine serum (FBS) (Gibco) and 1% penicillin and streptomycin (PEST) (Gibco) at 37 °C in a humidified incubator containing 5% carbon dioxide.

SH-SY5Y cells were differentiated using the following differentiation protocol: cells were plated on 6-well plates and were pre-differentiated on the next day with 10 μM RA in full media for 4 days. On the sixth day, 50 ng/ml of BDNF (Alomone Labs) in serum-free media was added for cell differentiation.

For ICP-MS and UHPLC experiments, cells were plated on 6-well plates 2 ml per well. Cells were plated with at least 2 x 10^6 cells/ml density. The Countess Automated Cell Counter instrument (Invitrogen) was used along with trypan blue stain for cell counting. 10 μl of cell suspension was mixed with 10 μl of trypan blue stain and pipetted into a chamber slide, which was inserted into the cell counter instrument.

For ICP-MS analysis, differentiated SH-SY5Y cells were supplemented with 5 μM $CuCl_2$ and 20 μM LA and incubated for 1, 2, 5, and 24 h.

For UHPLC analysis, differentiated SH-SY5Y cells were supplemented with 20 μM or 100 μM LA and incubated for 2, 5, and 24 h.

3.2.2 ICP-MS method

Sample preparation

Cells were washed with the media from the 6-well plates into nitric acid-washed 2 ml Eppendorf tubes and centrifuged for 1 min at 10 000 rpm to separate the media from the cells. 100 μl of supernatant was then pipetted into separate nitric acid-washed Eppendorf tubes as media samples for the ICP-MS analysis. The remaining media was then removed with vacuum aspiration. Cells were washed twice in 500 μl of phosphate-buffered saline (PBS), mixed using a vortex mixer, and centrifuged for 3 min at 10 000 rpm (this step was performed twice). After the second wash, cell counting was performed using 10 μl of cell suspension, as described in 3.2.1. PBS was removed with vacuum aspiration, and samples were stored at -20 °C until the ICP-MS analysis.

One day before the ICP-MS analysis, 100 μl of 68% HNO_3 was added to the cell and media samples. Samples with nitric acid were then incubated at room temperature for 24 h, after which they were centrifuged and diluted to 3,4% HNO_3 with ultrapure water.

Instrumentation

ICP-MS analyses were performed using Agilent Technologies (Santa Clara, USA) Agilent 7800 series ICP-MS instrument (Agilent, USA) in peak-hopping mode, 6 points per peak, 100 scans per replicate, and 5 replicates per sample. Agilent SPS-4 autosampler (Agilent Technologies, USA) was used for sample introduction. ICP-MS MassHunter 4.4 software Version C.01.04 from Agilent was used for instrument control and data acquisition. ICP-MS was operated under general matrix working mode under the following conditions: RF power 1550 W, nebulizer gas flow 1.05 l/min, plasma gas flow 15 l/min, nebulizer type: MicroMist. Elements monitored: Sc-45, Ge-72 (internal standard), Mn-55, Fe-56, Cu-63 and Zn-66.

Ultrapure water with a resistivity of 18.2 MΩ/cm, produced by a Merck Direct-Q & Direct–Q UV water purification system (Merck KGaA, Darmstadt, Germany), was used for all sample preparations. The ICP-MS apparatus was calibrated using 2% HNO_3 multielement calibration standard 2A (Agilent Technologies, USA) containing Ag, Al, As, Ba, Be, Ca, Cd, Co, Cr, Cs, Cu, Fe, Ga, K, Li, Mg, Mn, Na, Ni, Pb, Rb, Se, Sr, Tl, U, V, Zn at levels 0.5, 1, 5, 10 and 50 ppb with Sc-45 and Ge-72 (ICP-MS internal standard mix 1 ug/mL in 2% HNO3, Agilent Technologies) as the internal standard for Mn-55, Fe-56, Cu-63, and Zn-66 isotopes.

3.2.3 UHPLC method

Sample preparation

Cells were washed with the media from the 6-well plates into 2 ml Eppendorf tubes and centrifuged for 1 min at 10 000 rpm to separate the media from the cells. 60 μl of supernatant was then pipetted into separate Eppendorf tubes as media samples for the UHPLC analysis. The remaining media was removed with vacuum aspiration. Cells were washed twice with 500 μl of PBS, mixed using a vortex mixer, and centrifuged for 3 min at 10 000 rpm.

The protocol for sample preparation is an adapted version from the article [87]. In short, 60 μl of 0,1 M sodium tetraborate containing 2 mM EDTA (pH=9.4) (STB) (Acros Organics) was added to Eppendorf tubes with cells, mixed using a vortex mixer, and the cell suspension was then transferred into 0.1 mL PCR tubes. Cell and media samples were stored at -20°C until the UHPLC analysis.

Before the analysis, cells were sonicated with BioRuptor Pico (Diagenode) (30 s on/off, 15 cycles). Cell and media samples were acidified with 3 μl of TFA (Riedel-de Haën) and incubated for 5 min, after which 60 μl of acetone ethyl acetate 1:1 mixture (Acetone EtOAc) was added. Samples were centrifuged for 5 min at 15 000 rpm, and the upper layers of the supernatant were collected and transferred to separate Eppendorf tubes. This step was repeated 3 times, after which the samples were placed in a vacuum desiccator for 1,5 h to 2 h. When the samples were dry, 60 μl of STB was added and labeled with 10 μl 160 mM of tris(2-carboxyethyl)phosphine (TCEP) (Acros Organics), which reduces disulfide bonds in proteins, and 10 μl of 40 mM 4-(aminosulfonyl)-7-fluoro-2,1,3-benzoxadiazole (ABD-F) (Tokyo Chemical Industry), which is used for the labeling of thiol groups. The samples were incubated for 10 min at room temperature and centrifuged for 10 min at 15 000 rpm. 60 μl of the eluate was injected into HPLC cone vials (Macherey-Nagel) and inserted into the instrument.

Instrumentation

A Shimadzu UHPLC system consisting of two LC-30AD pumps, a CBM-20A system controller, an autosampler (SIL-30AC), and a degasser (DGU-20A_{5R}) was used. The analytical column for reversed-phase chromatography was Kinetex 2.6u C18 100A (150 mm x 4,6 mm i.d.; Phenomenex). The column was maintained at 40 °C by a CTO-20AC column oven (Shimadzu). The effluent was monitored by SPD-20A UV/vis and RF-20A_{XS} fluorescence detectors. The fluorescence detector was set at 380 nm (excitation) and 510 nm (emission). A linear gradient elution from H_2O-CH_3CN (95:5) containing 0,1% TFA to H_2O-CH_3CN (5:95) containing 0,1% TFA over 30 min was adapted. The flow rate of the mobile phase was 0.5 ml/min. The peak areas obtained from both detectors were calculated using LabSolutions software version 5.42 (Shimadzu).

3.2.4 *Drosophila melanogaster* cultivation, crossing and used strains

Fruit flies were cultured in plastic vials covered with foam plugs and filled to approximately ¼ with semolina-based food. Food consisted of 6,5 g agar, 38 g semolina, 70,5 g malt flour, 17,5 g dry yeast, 5,9 ml nipagin (Tegosept 30%; 30g/100ml 94% EtOH; Dutcher Scientific), and 6,8 ml propionic acid (Sigma) per 1000 ml water. Water, agar, semolina, and malt flour were mixed and boiled for 10 min, after which the yeast was added. The food was then cooled down to 70 °C, and nipagin and propionic acid were added to avoid mold and bacterial growth.

$CuCl_2$ was dissolved in 0,5% HCl at 1 M concentration and added to the food with a final concentration of 500 μM (Cu-food). Control food contained the same amount of 0,5% HCl used to produce the food supplemented with $CuCl_2$ (food). LA was dissolved in EtOH at 200 mM concentration and added to food with a final concentration of 2 mM in the presence of 500 μM $CuCl_2$ (Cu/LA food). Food supplemented with EtOH has already been used in experiments by our group, and it did not have any effect on the locomotor activity or longevity of fruit flies.

Flies were maintained in incubators with 12 h light and dark cycle with 60% humidity. Flies were kept at 18 °C for stocks, 25 °C, and 29 °C for experiments.

As a responder line to generate transgenic models for AD, UAS-APP695-N-myc, UAS-BACE1/TM6B (Vitruvian; Bloomington Drosophila Stock Center (BDSC) #33797) overexpressing human APP and BACE1 was used. As a driver line, eye-specific *ninaE^{GMR}-Gal4* (BDSC, #1104) was used to activate the transgene.

For crossings, 10-15 virgin females of the responder line were crossed with 5-7 males of the driver line. Vials were kept at a 29 °C incubator for a higher Gal4 effect. After 4-5 days, parents were removed from vials, and after 9-11 days, transgenic flies were collected for the experiment.

For the eye phenotype experiment, flies were kept on Cu-food and food from the egg stage. Within 24 h after eclosion, half of the adult flies kept on Cu-food were transferred to Cu/LA-food. Scanning electron microscopy (SEM) was used for imaging fly eyes on days 5, 10, and 20 after hatching.

3.2.5 Statistical analysis

Statistical analyses for data obtained from ICP-MS were performed using GraphPad Prism version 9.3.1. One-way ANOVA was followed by the post hoc Dunnett's multiple comparisons test. The figures display the mean ± SEM. Statistical significance of $p \leq 0,05$ is represented as *, $p \leq 0,01$ as **, $p \leq 0,001$ as ***, and $p \leq 0,0001$ as ****.

4 Results

4.1 The kinetics of LA-induced copper transport studied by ICP-MS

To investigate the kinetics of LA-induced copper transport, timepoint experiments using ICP-MS were performed. Differentiated SH-SY5Y cells were collected 1 h, 2 h, 5 h, and 24 h after treatment with 5 μM $CuCl_2$ and 20 μM LA. The results of these experiments are presented in Figure 4. No significant changes in copper levels were detected until the 5 h timepoint (Figure 4C), in which a modest increase occurred. Copper levels increased significantly in the presence of LA after 24 h incubation (Figure 4D).

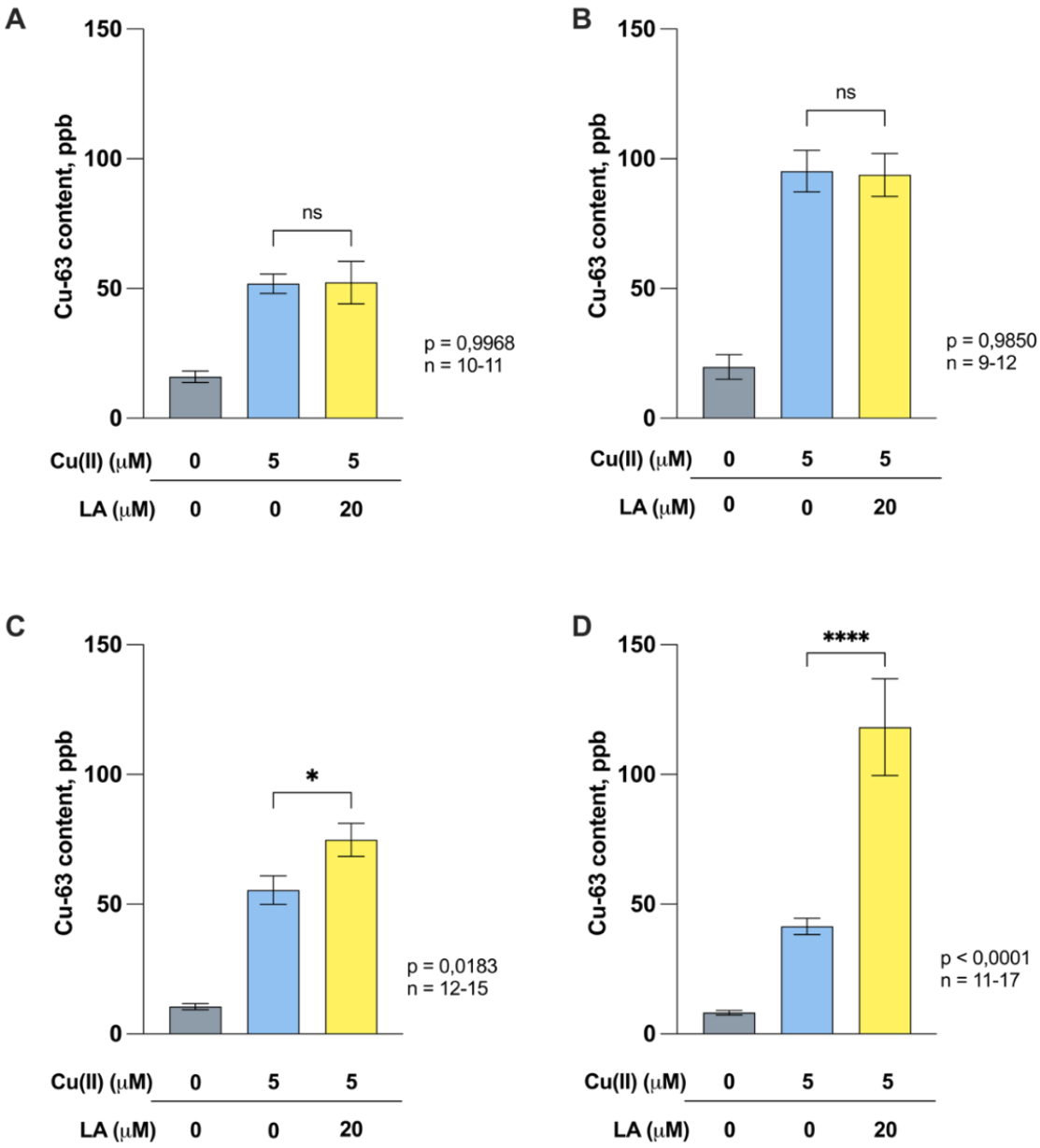

Figure 4. ICP-MS analysis of Cu^{2+} ions distribution between media and cells at timepoints 1h, 2h, 5h and 24h. The figure depicts Cu-63 content in untreated cells vs. cells treated with 5 μM $CuCl_2$ and 20 μM LA at **(A)** 1 h, **(B)** 2 h, **(C)** 5 h, and **(D)** 24 h timepoints. The figure displays the mean ± SEM; n = 9-17. One-way ANOVA followed by Dunnett's multiple comparisons test at the 0,05 level was used for statistical analysis.

4.2 Cellular LA accumulation studied by UHPLC

To investigate the kinetics of cellular LA accumulation, timepoint experiments using UHPLC were performed. Differentiated SH-SY5Y cells and media samples were collected 2 h, 5 h, and 24 h after treatment with 20 μM or 100 μM LA. The results of these experiments are presented in Figures 5, 6, and 7.

Media samples supplemented with 20 μM and 100 μM LA showed a gradual decrease in LA concentration in 2 to 5 h after treatment. However, the concentration increased again at 24 h after treatment (Figure 5B, Figure 5C).

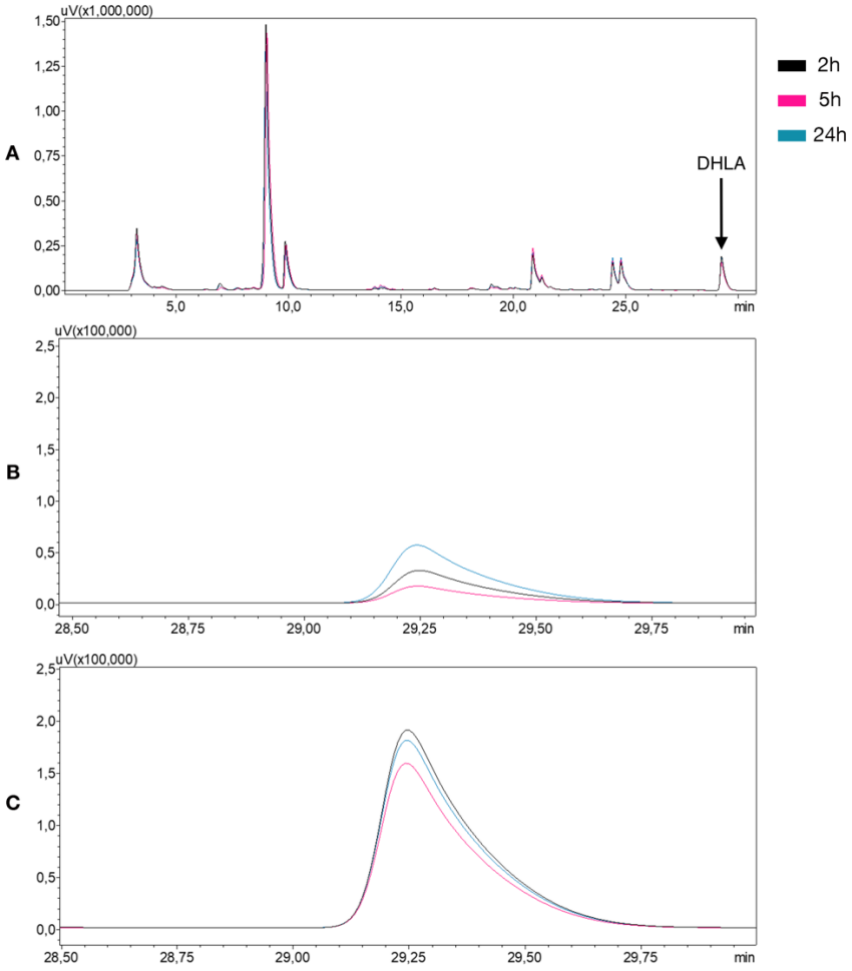

Figure 5. UHPLC analysis of LA-treated cell media samples. Media samples were collected 2 h (black), 5 h (red), and 24 h (blue) after supplementation with 20 μM or 100 μM LA. (**A**) Full-sized chromatogram showing all obtained peaks from the LA-treated medium. The retention time for LA was between 29 and 30 min. Magnification of the LA peak in medium treated with 20 μM LA (**B**) and 100 μM LA (**C**).

Cellular LA accumulation was only detected in cells collected 5 h after supplementation and showed a higher concentration when supplemented with 100 μM LA than 20 μM LA (Figure 6B, E). In some experiments, LA was also detected in cells 24 h after supplementation.

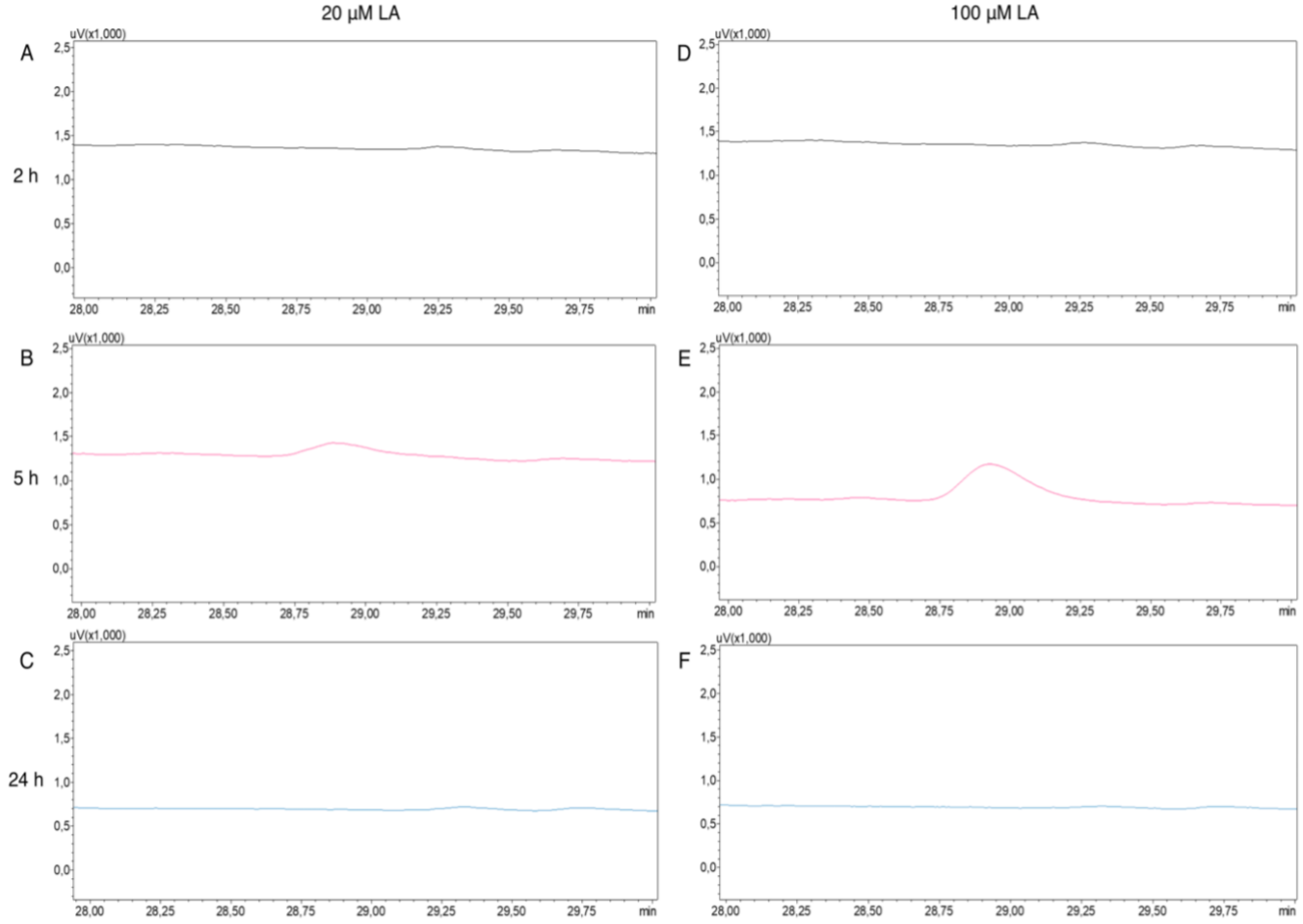

Figure 6. UHPLC analysis of LA-treated cell samples. Cell samples were collected 2 h (**A**, **D**), 5 h (**B**, **E**), and 24 h (**C**, **F**) after supplementation with 20 μM (**A**-**C**) and 100 μM LA (**D**-**F**).

Calibration was performed during every experiment and one calibration curve is presented in Figure 8. The corresponding peaks of the calibration curve are presented in Figure 7.

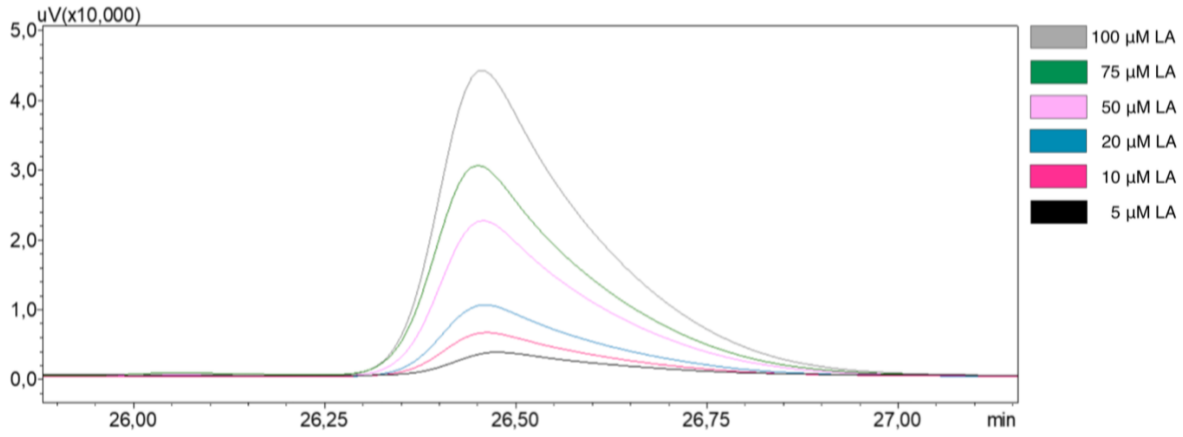

Figure 7. LA peaks of calibration solutions. Calibration was performed using LA concentrations of 5 µM (black), 10 µM (red), 20 µM (blue), 50 µM (pink), 75 µM (green), and 100 µM (grey).

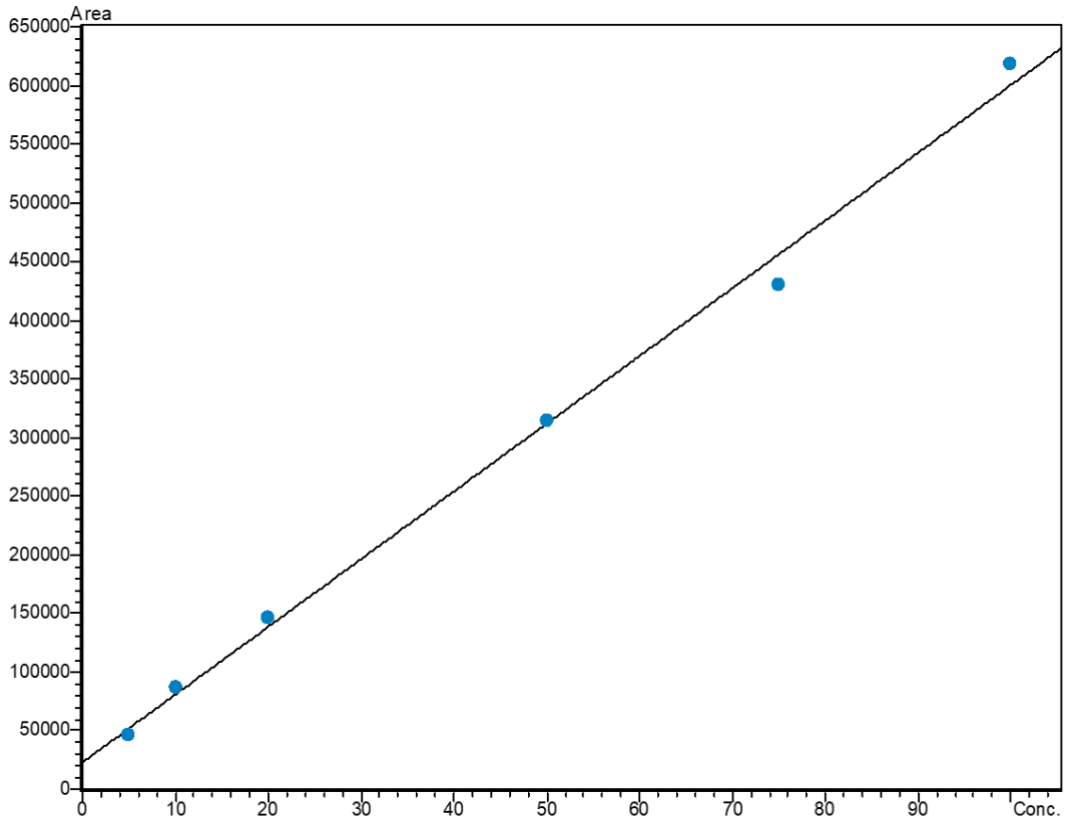

Figure 8. Calibration curve of LA. The retention time for LA was 26,451; R^2=0,995; y=5772,9*x+23358,8. The calibration curve was constructed using LabSolutions software version 5.42 (Shimadzu).

4.3 LA effect on copper-induced neurodegeneration in APP/Bace1 AD *Drosophila* model

To investigate the effect of LA on copper-induced neurodegeneration, SEM examinations were performed on fruit flies with eye-specific human APP and Bace1 overexpression. Fruit flies were kept on food and Cu-food from the egg-laying stage, and half of the flies kept on Cu-food were transferred to Cu/LA-food within 24 h from hatching. SEM examinations were performed on days 5, 10, and 20 after hatching. The results of these experiments are presented in Figure 9. APP/Bace1 flies developed irregular compound eyes with a smooth phenotype (Figure 9D-L) compared to the normal bristled ommatidia compound eyes of control flies (Figure 9A-C). APP/Bace1 flies kept on Cu-food developed dark deposits mainly in the corners of the eye, which were exacerbated in time (Figure 9E, H, K). The addition of LA into the food prevented the exacerbation of dark deposits (Figure 9F, I, L).

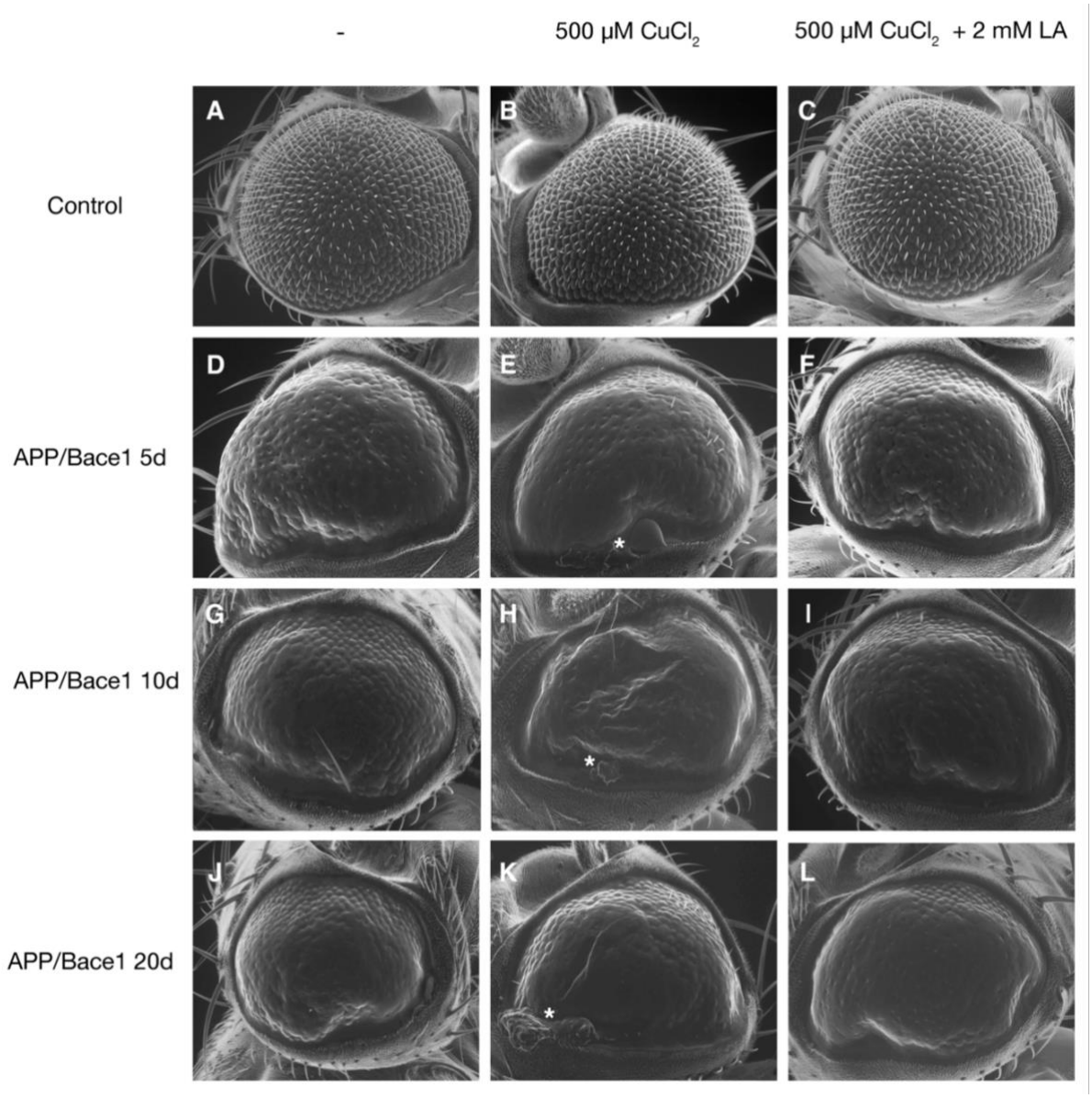

Figure 9. The effect of LA on copper-induced neurodegeneration in eye-specific APP/Bace1 overexpression in *Drosophila melanogaster* AD models. The figure represents SEM images of eye morphology of *ninaE*^{GMR}*-Gal4/+;TM6B* flies as control (**A-C**), and APP/Bace1 AD flies (**D-L**) on days 5 (**D-F**), 10 (**G-I**), and 20 (**J-L**). Flies were kept on food, Cu-food, and Cu/LA-food. Dark deposits are marked on the figure with asterisks (**E**, **H, K**).

5 Discussion

Copper metabolism is altered in the case of AD. Copper concentrations are high in amyloid plaques, as Cu(II) ions bind to Aβ peptides and induce their aggregation process. At the same time, cells are in copper deficiency, particularly in brain regions most affected by the disease, e.g., the hippocampus and amygdala. Thus, there is a need for a copper-regulating ligand, which could induce the relocation of copper ions from the extracellular into the intracellular environment and restore normal cellular functioning. Recently, we proposed using LA, a natural ligand with a relatively strong affinity for Cu(I) ions. Other metal chelators tested, such as CQ and PBT-2, are synthetic Cu(II)-binding compounds that did not exhibit significant effects in clinical trials [88]. Synthetic chelators may also excrete copper ions from the body, harming AD patients as the brain tissue is already in copper deficiency.

Our group has shown that LA can redistribute copper ions from the extracellular into the intracellular environment. However, the mechanism of LA action on copper metabolism has not yet been investigated. Intracellularly, DHLA may directly bind Cu(I) ions and affect copper balance by promoting copper influx into the cell. Importantly, DHLA has a relatively strong affinity for Cu(I) ions, however, it does not demetallate essential copper-binding proteins. It is known that LA increases glutathione synthesis and acts as an antioxidant [89], which may also positively affect copper metabolism. Alternatively, LA may indirectly affect the regulation of copper metabolism by enhancing or suppressing the synthesis of some proteins.

Importantly, LA has been evaluated in an open and non-randomized study for AD patients with mild to moderate cognitive impairment [90]. The results showed, that LA was able to slow the progression of cognitive impairment, however, as the mechanism of action is not elucidated, the trials have not been taken further on. This may be due to the fact, that the positive effects were attributed to LA as an antioxidant. It is utterly important to understand how the therapeutic agent works. In this study, it was shown that LA may have an effect as a copper redistributing agent. By restoring normal copper metabolism, cellular energy production improves, and copper availability enhances the synthesis of SOD1, which ameliorates oxidative stress that also occurs in the AD brain.

Hereby, one of the aims of this work was to study the kinetics of LA action on copper redistribution. This was realized by measuring copper content in copper and LA supplemented differentiated SH-SY5Y cells at different timepoints by using ICP-MS. A slight increase in copper levels was detected 5 h after treatment with 20 μM LA in the presence of 5 μM $CuCl_2$ and a significant increase was detected 24 h after treatment. Hence, LA has a relatively slow action on copper redistribution.

In parallel with copper measurements, we also investigated the kinetics of cellular LA accumulation in supplemented SH-SY5Y cells by using UHPLC according to the protocol presented in 3.4. LA accumulation was detected in cells collected 5 h and 24 h after supplementation, but we did not see those peaks in every experiment performed. It could be caused by a lower cell count or some parameter of UHPLC. Nevertheless, these results show that LA accumulation is faster than copper

redistribution. Such a result suggests that LA may indirectly affect the regulation of copper metabolism by enhancing or suppressing the synthesis of some proteins. Further proteomics studies are needed to elucidate the changes in the proteome of cells after LA treatment. An initial decrease and later increase in LA concentration in the medium was detected, which is difficult to explain and requires additional experimentation. The method used in this study [87] needs further improvement as the results obtained were, in many cases, contradictory.

We have previously shown that LA positively affects the locomotor activity of transgenic AD model flies. To study the effect of LA on copper-induced neurodegeneration, transgenic AD model flies with eye-specific human APP and Bace1 overexpression were used. SEM images showed that the addition of Cu(II) ions into food caused the formation of dark deposits in the case of AD flies, which were exacerbated in time. The supplementation with 20 μM LA in the presence of Cu(II) ions inhibited the exacerbation of dark deposits, which demonstrates a protective role of LA on copper-induced neurodegeneration. Initial results of this experiment were also published in our recent paper [68].

Taken together, the results of this study have shown that LA likely affects copper metabolism by regulating protein synthesis, which should be further confirmed by proteomics studies. LA also has an *in vivo* protective effect on copper-induced neurodegeneration in AD model flies with eye-specific human APP and Bace1 overexpression.

Abstract

Alzheimer's disease (AD) is a neurodegenerative disorder that results in cognitive decline. The pathological hallmarks of AD are extracellular amyloid plaques and intracellular neurofibrillary tangles. Many hypotheses have been proposed for AD, yet the exact cause of the disease remains unknown. The most researched theory is the amyloid cascade, which postulates that the amyloid-β (Aβ) peptide, which is the principal constituent of amyloid plaques, is the causative factor of AD. According to the amyloid cascade, Aβ peptides accumulate and form plaques, followed by the formation of intracellular neurofibrillary tangles, consisting of hyperphosphorylated tau protein, leading to neuronal death.

In the AD brain, copper ions bind to Aβ peptides and induce their aggregation. Therefore, copper concentrations are high in amyloid plaques, leaving the cells deficient and resulting in copper dyshomeostasis. There is a need to restore the normal copper metabolism by finding a copper-regulating ligand that could relocate copper ions into copper-deficient cells. Previously, synthetic chelators have been tested in clinical trials, however, some have been found toxic or without any clinical benefit. We propose a natural ligand, α-lipoic acid (LA), which has a relatively strong affinity for Cu(I) ions and has been shown to redistribute copper ions from the extracellular into the intracellular environment. We have also demonstrated that LA improves the locomotor activity of transgenic AD *Drosophila* models, however, the mechanism of LA action on copper metabolism has not been investigated.

This study investigated the kinetics of LA-promoted copper transport in differentiated SH-SY5Y cell culture using ICP-MS. A slight increase of copper content was detected in LA-supplemented cells in the presence of Cu(II) ions 5 h after supplementation, and a significant increase occurred 24 h after supplementation. The results showed that the action of LA on copper redistribution is rather slow.

To further understand if LA directly participates in copper redistribution, cellular accumulation of LA was studied in differentiated SH-SY5Y cells using UHPLC. Results show that LA could be detected in cells 5 h and 24 h after supplementation. LA concentration in the medium first decreased and then increased, which remains questionable and needs further investigation.

The effect of LA was also investigated on copper-induced neurodegeneration when human APP and Bace1 were overexpressed eye-specifically in AD fruit fly model. Dark deposits were observed on compound eyes when flies were incubated on Cu(II)-supplemented food, which exacerbated in time. The supplementation with LA in the presence of Cu(II) ions inhibited the exacerbation of dark deposits, which indicates that LA has a protective role in copper-induced neurodegeneration.

These results show that LA likely affects copper metabolism by regulating protein synthesis. Further investigation into proteomics of LA-treated cells should be performed. LA also has an *in vivo* effect on copper-induced neurodegeneration in AD fruit fly model.

Annotatsioon

Alzheimeri tõbi (AT) on progressiivne neurodegeneratiivne haigus ja peamine dementsuse põhjustaja. Haigust kirjeldati esmakordselt 1906. aastal Alois Alzheimeri poolt, kelle järgi sai haigus ka nime. AT peamisteks tunnusteks on ekstratsellulaarsete amüloidsete naastude ja intratsellulaarsete neurofibrillaarsete kämpude esinemine ajus. Amüloidsed naastud koosnevad agregeerunud amüloid-β (Aβ) peptiididest ning neurofibrillaarsete kämpude koostiseks on hüperfosforüleeritud tau valk. Hetkel on maailmas ligi 55 miljonit dementsusest mõjutatud inimest ning Maailma Terviseorganisatsiooni andmetel on dementsus seitsmes juhtiv surmapõhjus.

Üle 90% AT juhtudest on sporaadilised, kuid esineb ka AT pärilikku vormi, mille puhul on mutatsioonid geenides, mis kodeerivad amüloidi eellasvalku (APP), presenilliin-1 (PSEN1) või presenilliin-2 (PSEN2) valke. AT sporaadilise vormi riski tõstab *APOE* geeni neljanda alleeli esinemine.

Kuigi AT on palju uuritud haigus, ei ole siiani tuvastatud haiguse tekkepõhjust. On välja pakutud mitmeid hüpoteese, millest tuntuim on amüloidse kaskaadi hüpotees. Amüloidse kaskaadi hüpotees viitab Aβ peptiidide agregeerumisele kui haiguse initseerijale, millele järgneb neurofibrillaarsete kämpude teke ning neurodegeneratsioon. Muude hüpoteeside hulka kuuluvad tau hüpotees, metallide hüpotees jne.

Ajul on kõrge energiavajadus, mistõttu on aju hapniku tarbimine oluliselt suurem võrreldes teiste organitega. Sellel põhjusel on ajus ka rohkem biometalle, mis on kofaktoriks või struktuurseks komponendiks erinevatele valkudele. AT puhul aga esinevad biometallide homeostaasi häired, mis on tõenäoliselt tingitud Aβ peptiidi agregaatide interaktsioonidest biometallide, aga peamiselt vase ioonidega. On näidatud, et amüloidsetes naastudes on vase ioonide kontsentratsioon kõrge, jättes rakud defitsiiti.

Haiguse raviks on välja pakutud palju ravimkandidaate, millest enim on suunatud amüloidile, kuid mis ei ole näidanud kliinilist efektiivsust. 2021. aastal kiideti heaks Aducanumab, amüloididele suunatud monoklonaalne antikeha, mille kliiniliste katsete tulemused on vastuolulised ning puudub selge suhe amüloidsete naastude vähenemise ja kognitiivsete võimete paranemise vahel. Seetõttu on üliloluline leida toimiv ravi, mis suudaks haigust ära hoida või selle kulgu peatada.

Tuginedes vase homöostaasi häire hüpoteesile, pakkusime välja naturaalse ligandi α-lipoehappe (LA), mis võiks normaliseerida vase metabolismi AT ajus. Meie grupp on varasemalt näidanud, et redutseeritud LA (DHLA) omab optimaalset afiinsust Cu(I) ioonidele ning paigutab vase ioone ekstratsellulaarsest keskkonnast intratsellulaarsesse. Meie hiljuti avaldatud artiklis on näidatud, et LA avaldab positiivset mõju transgeensete AT äädikakärbeste lokomotoorsele aktiivsusele. Varasemalt on samuti LA-d selle neuroprotektiivsete omaduste tõttu AT raviks välja pakutud, kuid LA toimimise mehhanismi pole siiani uuritud.

Antud töös uuriti LA mõju vase transpordi kineetikale erinevatel ajapunktidel (1 h, 2 h, 5 h ja 24 h) pärast Cu(II) ioonide ja LA lisamist diferentseeritud SH-SY5Y rakkudele kasutades ICP-MS tehnoloogiat. Vase tasemetes oli näha vähest tõusu 5 h möödudes, kuid statistiliselt oluline tõus esines 24 h möödudes. Antud tulemusest nähtub, et LA mõju vase transpordile on üsna aeglane.

Lisaks uuriti UHPLC tehnoloogia abil LA akumulatsiooni diferentseeritud SH-SY5Y rakkudes ajapunktidel 2 h, 5 h, ja 24 h pärast LA lisamist. LA piike õnnestus näha rakkudes 5 h ja 24 h möödumisel LA lisamisest, kuid mitte iga kord. Tõenäoliselt sõltub see rakkude hulgast või mõnest UHPLC parameetrist. Lisaks oli näha söötmes algselt LA kontsentratsiooni langust võrreldes 2 h ja 5 h ajapunkte, ning seejärel kontsentratsiooni tõusu 24 h juures, mida on keeruline selgitada. Antud töös kasutatud meetod vajab kindlasti parendamist ja projekt edasist eksperimenteerimist. Sellest olenemata nähtub, et LA akumulatsioon on rakkudes kiirem kui selle mõju vase transpordile, millest võib järeldada, et LA võiks mõjutada vase metabolismi reguleerides valkude sünteesi.

Antud töös uuriti ka LA mõju vask-indutseeritud neurodegeneratsioonile transgeensetes inimese APP ja Bace1 fotoretseptor-spetsiifiliselt ekspresseerivas AT äädikakärbse mudelis kasutades skanneerivat elektronmikroskoopiat. Äädikakärbseid hoiti vasega rikastatud toidul (Cu-toit) ning toidul alates embrüo staadiumist. Täiskasvanuks saades jaotati Cu-toidul inkubeeritud äädikakärbsed Cu-toidu ning vase ja LA-ga rikastatud toidu (Cu/LA-toit) vahel. Äädikakärbeste silmi pildistati 5., 10., ja 20. päeval peale nukust koorumist. APP/Bace1 Cu-toidul inkubeeritud äädikakärbestel tekkisid silmadele tumedad laigud, mis ajaga progresseerusid. LA lisamine toidule aitas ära hoida nende laikude progresseerumise, mis näitab, et LA omab kaitsvat rolli vask-indutseeritud neurodegeneratsioonile. Antud katse eeltulemused on avaldatud ka meie poolt publitseeritud artiklis [68].

Antud töö tulemustest võib järeldada, et LA mõju vase ümberjaotamisele rakuvälise ja –sisese keskkonna vahel on üsna aeglane protsess, kuid LA akumulatsioon rakkudesse on kiirem. Kindlasti tuleks teostada proteoomika analüüs, mis annaks kinnitust, kas LA võiks toimida vase metabolismile valkude sünteesi reguleerimise kaudu.

Acknowledgments

I would like to thank my supervisors, Sigrid Kirss and professor Peep Palumaa for their knowledge and support throughout my master's studies. I would also like to thank Katrina Laks for helping to perform the ICP-MS analysis and all other members of our Metalloproteomics group.

I am also very grateful to Mari Palgi and Laura Tamberg from the Molecular Neurobiology research group for their help with SEM experiments and for always giving advice regarding fruit fly experiments.

References

1. Moller, H.J. and M.B. Graeber, *The case described by Alois Alzheimer in 1911. Historical and conceptual perspectives based on the clinical record and neurohistological sections.* Eur Arch Psychiatry Clin Neurosci, 1998. **248**(3): p. 111-22.
2. Organization, W.H. *Dementia*. 2021 [cited 2022 12.02]; Available from: https://www.who.int/news-room/fact-sheets/detail/dementia.
3. Wang, X., M.L. Michaelis, and E.K. Michaelis, *Functional genomics of brain aging and Alzheimer's disease: focus on selective neuronal vulnerability.* Curr Genomics, 2010. **11**(8): p. 618-33.
4. Alzheimer's, A., *2016 Alzheimer's disease facts and figures.* Alzheimers Dement, 2016. **12**(4): p. 459-509.
5. Buxbaum, J.D., et al., *Alzheimer amyloid protein precursor in the rat hippocampus: transport and processing through the perforant path.* J Neurosci, 1998. **18**(23): p. 9629-37.
6. Priller, C., et al., *Synapse formation and function is modulated by the amyloid precursor protein.* J Neurosci, 2006. **26**(27): p. 7212-21.
7. Zhang, X. and W. Song, *The role of APP and BACE1 trafficking in APP processing and amyloid-beta generation.* Alzheimers Res Ther, 2013. **5**(5): p. 46.
8. Nunan, J. and D.H. Small, *Regulation of APP cleavage by alpha-, beta- and gamma-secretases.* FEBS Lett, 2000. **483**(1): p. 6-10.
9. Serrano-Pozo, A., et al., *Neuropathological alterations in Alzheimer disease.* Cold Spring Harb Perspect Med, 2011. **1**(1): p. a006189.
10. Ringman, J.M., et al., *Genetic heterogeneity in Alzheimer disease and implications for treatment strategies.* Curr Neurol Neurosci Rep, 2014. **14**(11): p. 499.
11. Sun, Q., et al., *Alzheimer's Disease: From Genetic Variants to the Distinct Pathological Mechanisms.* Front Mol Neurosci, 2017. **10**: p. 319.
12. Steiner, H., R. Fluhrer, and C. Haass, *Intramembrane proteolysis by gamma-secretase.* J Biol Chem, 2008. **283**(44): p. 29627-31.
13. Cacace, R., K. Sleegers, and C. Van Broeckhoven, *Molecular genetics of early-onset Alzheimer's disease revisited.* Alzheimers Dement, 2016. **12**(6): p. 733-48.
14. Dimitrov, M., et al., *Alzheimer's disease mutations in APP but not gamma-secretase modulators affect epsilon-cleavage-dependent AICD production.* Nat Commun, 2013. **4**: p. 2246.
15. Mendez, M.F., *Early-Onset Alzheimer Disease.* Neurol Clin, 2017. **35**(2): p. 263-281.
16. Farrer, L.A., et al., *Effects of age, sex, and ethnicity on the association between apolipoprotein E genotype and Alzheimer disease. A meta-analysis. APOE and Alzheimer Disease Meta Analysis Consortium.* JAMA, 1997. **278**(16): p. 1349-56.
17. Silva, M.V.F., et al., *Alzheimer's disease: risk factors and potentially protective measures.* J Biomed Sci, 2019. **26**(1): p. 33.
18. Hardy, J. and D. Allsop, *Amyloid deposition as the central event in the aetiology of Alzheimer's disease.* Trends Pharmacol Sci, 1991. **12**(10): p. 383-8.
19. Liu, P.P., et al., *History and progress of hypotheses and clinical trials for Alzheimer's disease.* Signal Transduct Target Ther, 2019. **4**: p. 29.
20. Wang, L., et al., *Current understanding of metal ions in the pathogenesis of Alzheimer's disease.* Transl Neurodegener, 2020. **9**: p. 10.
21. Floyd, R.A., *Antioxidants, oxidative stress, and degenerative neurological disorders.* Proc Soc Exp Biol Med, 1999. **222**(3): p. 236-45.

22. Hare, D., et al., *A delicate balance: Iron metabolism and diseases of the brain.* Front Aging Neurosci, 2013. **5**: p. 34.
23. Singh, A., et al., *Oxidative Stress: A Key Modulator in Neurodegenerative Diseases.* Molecules, 2019. **24**(8).
24. Connor, J.R., et al., *A histochemical study of iron, transferrin, and ferritin in Alzheimer's diseased brains.* J Neurosci Res, 1992. **31**(1): p. 75-83.
25. Hallgren, B. and P. Sourander, *The effect of age on the non-haemin iron in the human brain.* J Neurochem, 1958. **3**(1): p. 41-51.
26. Ward, R.J., et al., *The role of iron in brain ageing and neurodegenerative disorders.* Lancet Neurol, 2014. **13**(10): p. 1045-60.
27. Maynard, C.J., et al., *Overexpression of Alzheimer's disease amyloid-beta opposes the age-dependent elevations of brain copper and iron.* J Biol Chem, 2002. **277**(47): p. 44670-6.
28. Coleman, J.E., *Zinc proteins: enzymes, storage proteins, transcription factors, and replication proteins.* Annu Rev Biochem, 1992. **61**: p. 897-946.
29. McCall, K.A., C. Huang, and C.A. Fierke, *Function and mechanism of zinc metalloenzymes.* J Nutr, 2000. **130**(5S Suppl): p. 1437S-46S.
30. Faller, P., La Penna, G., Hureau, C., Furlan, S., *Coordination of Metal Ions to ß-Amyloid Peptide: Impact on Alzheimer's Disease*, in *Alzheimer's Disease: Insights into Low Molecular Weight and Cytotoxic Aggregates from In Vitro and Computer Experiments*, P. Derreumaux, Editor. 2013: Imperial College Press. p. 127-155.
31. Mezzaroba, L., et al., *The role of zinc, copper, manganese and iron in neurodegenerative diseases.* Neurotoxicology, 2019. **74**: p. 230-241.
32. Lei, P., S. Ayton, and A.I. Bush, *The essential elements of Alzheimer's disease.* J Biol Chem, 2021. **296**: p. 100105.
33. Lovell, M.A., et al., *Copper, iron and zinc in Alzheimer's disease senile plaques.* J Neurol Sci, 1998. **158**(1): p. 47-52.
34. Huang, X., et al., *The A beta peptide of Alzheimer's disease directly produces hydrogen peroxide through metal ion reduction.* Biochemistry, 1999. **38**(24): p. 7609-16.
35. Lewinska-Preis, L., et al., *Bioelements and mineral matter in human livers from the highly industrialized region of the Upper Silesia Coal Basin (Poland).* Environ Geochem Health, 2011. **33**(6): p. 595-611.
36. Scheiber, I.F., J.F. Mercer, and R. Dringen, *Metabolism and functions of copper in brain.* Prog Neurobiol, 2014. **116**: p. 33-57.
37. Davies, K.M., et al., *Localization of copper and copper transporters in the human brain.* Metallomics, 2013. **5**(1): p. 43-51.
38. Fu, S., W. Jiang, and W. Zheng, *Age-dependent increase of brain copper levels and expressions of copper regulatory proteins in the subventricular zone and choroid plexus.* Front Mol Neurosci, 2015. **8**: p. 22.
39. Tarohda, T., M. Yamamoto, and R. Amamo, *Regional distribution of manganese, iron, copper, and zinc in the rat brain during development.* Anal Bioanal Chem, 2004. **380**(2): p. 240-6.
40. James, S.A., et al., *Elevated labile Cu is associated with oxidative pathology in Alzheimer disease.* Free Radic Biol Med, 2012. **52**(2): p. 298-302.
41. Deibel, M.A., W.D. Ehmann, and W.R. Markesbery, *Copper, iron, and zinc imbalances in severely degenerated brain regions in Alzheimer's disease: possible relation to oxidative stress.* J Neurol Sci, 1996. **143**(1-2): p. 137-42.
42. Fasae, K.D., et al., *Metallobiology and therapeutic chelation of biometals (copper, zinc and iron) in Alzheimer's disease: Limitations, and current and future perspectives.* J Trace Elem Med Biol, 2021. **67**: p. 126779.
43. Bush, A.I., *Drug development based on the metals hypothesis of Alzheimer's disease.* J Alzheimers Dis, 2008. **15**(2): p. 223-40.

44. Sarell, C.J., et al., *Copper(II) binding to amyloid-beta fibrils of Alzheimer's disease reveals a picomolar affinity: stoichiometry and coordination geometry are independent of Abeta oligomeric form.* Biochemistry, 2009. **48**(20): p. 4388-402.
45. Matheou, C.J., N.D. Younan, and J.H. Viles, *Cu(2)(+) accentuates distinct misfolding of Abeta(1)(-)(4)(0) and Abeta(1)(-)(4)(2) peptides, and potentiates membrane disruption.* Biochem J, 2015. **466**(2): p. 233-42.
46. Hureau, C. and P. Faller, *Abeta-mediated ROS production by Cu ions: structural insights, mechanisms and relevance to Alzheimer's disease.* Biochimie, 2009. **91**(10): p. 1212-7.
47. Wu, W.H., et al., *Sequestration of copper from beta-amyloid promotes selective lysis by cyclen-hybrid cleavage agents.* J Biol Chem, 2008. **283**(46): p. 31657-64.
48. Cummings, J., et al., *Alzheimer's disease drug development pipeline: 2021.* Alzheimers Dement (N Y), 2021. **7**(1): p. e12179.
49. Tampi, R.R., B.P. Forester, and M. Agronin, *Aducanumab: evidence from clinical trial data and controversies.* Drugs Context, 2021. **10**.
50. Cummings, J.L., G. Tong, and C. Ballard, *Treatment Combinations for Alzheimer's Disease: Current and Future Pharmacotherapy Options.* J Alzheimers Dis, 2019. **67**(3): p. 779-794.
51. Cherny, R.A., et al., *Aqueous dissolution of Alzheimer's disease Abeta amyloid deposits by biometal depletion.* J Biol Chem, 1999. **274**(33): p. 23223-8.
52. Kaur, D., et al., *Genetic or pharmacological iron chelation prevents MPTP-induced neurotoxicity in vivo: a novel therapy for Parkinson's disease.* Neuron, 2003. **37**(6): p. 899-909.
53. Sales, T.A., et al., *Recent Developments in Metal-Based Drugs and Chelating Agents for Neurodegenerative Diseases Treatments.* Int J Mol Sci, 2019. **20**(8).
54. Adlard, P.A., et al., *Rapid restoration of cognition in Alzheimer's transgenic mice with 8-hydroxy quinoline analogs is associated with decreased interstitial Abeta.* Neuron, 2008. **59**(1): p. 43-55.
55. Bast, A. and G.R. Haenen, *Lipoic acid: a multifunctional antioxidant.* Biofactors, 2003. **17**(1-4): p. 207-13.
56. Theodosis-Nobelos, P., et al., *Lipoic acid. Kinetics and pluripotent biological properties and derivatives.* Mol Biol Rep, 2021. **48**(9): p. 6539-6550.
57. Salehi, B., et al., *Insights on the Use of alpha-Lipoic Acid for Therapeutic Purposes.* Biomolecules, 2019. **9**(8).
58. Maczurek, A., et al., *Lipoic acid as an anti-inflammatory and neuroprotective treatment for Alzheimer's disease.* Adv Drug Deliv Rev, 2008. **60**(13-14): p. 1463-70.
59. Handelman, G.J., et al., *Alpha-lipoic acid reduction by mammalian cells to the dithiol form, and release into the culture medium.* Biochem Pharmacol, 1994. **47**(10): p. 1725-30.
60. Scott, B.C., et al., *Lipoic and dihydrolipoic acids as antioxidants. A critical evaluation.* Free Radic Res, 1994. **20**(2): p. 119-33.
61. Bilska, A., et al., *Alpha-lipoic acid differently affects the reserpine-induced oxidative stress in the striatum and prefrontal cortex of rat brain.* Neuroscience, 2007. **146**(4): p. 1758-71.
62. Haugaard, N. and R.M. Levin, *Activation of choline acetyl transferase by dihydrolipoic acid.* Mol Cell Biochem, 2002. **229**(1-2): p. 103-6.
63. Holmquist, L., et al., *Lipoic acid as a novel treatment for Alzheimer's disease and related dementias.* Pharmacol Ther, 2007. **113**(1): p. 154-64.
64. Kaur, D., et al., *Decrypting the potential role of alpha-lipoic acid in Alzheimer's disease.* Life Sci, 2021. **284**: p. 119899.
65. Staykov, H., et al., *Neuromodulatory Mechanisms of a Memory Loss-Preventive Effect of Alpha-Lipoic Acid in an Experimental Rat Model of Dementia.* J Mol Neurosci, 2022.
66. Quinn, J.F., et al., *Chronic dietary alpha-lipoic acid reduces deficits in hippocampal memory of aged Tg2576 mice.* Neurobiol Aging, 2007. **28**(2): p. 213-25.

67. Smirnova, J., et al., *Copper(I)-binding properties of de-coppering drugs for the treatment of Wilson disease. alpha-Lipoic acid as a potential anti-copper agent.* Sci Rep, 2018. **8**(1): p. 1463.
68. Metsla, K., et al., *alpha-Lipoic Acid Has the Potential to Normalize Copper Metabolism, Which Is Dysregulated in Alzheimer's Disease.* J Alzheimers Dis, 2022. **85**(2): p. 715-728.
69. Ross, R.A., B.A. Spengler, and J.L. Biedler, *Coordinate morphological and biochemical interconversion of human neuroblastoma cells.* J Natl Cancer Inst, 1983. **71**(4): p. 741-7.
70. Kovalevich, J. and D. Langford, *Considerations for the use of SH-SY5Y neuroblastoma cells in neurobiology.* Methods Mol Biol, 2013. **1078**: p. 9-21.
71. Encinas, M., et al., *Sequential treatment of SH-SY5Y cells with retinoic acid and brain-derived neurotrophic factor gives rise to fully differentiated, neurotrophic factor-dependent, human neuron-like cells.* J Neurochem, 2000. **75**(3): p. 991-1003.
72. Jamsa, A., et al., *The retinoic acid and brain-derived neurotrophic factor differentiated SH-SY5Y cell line as a model for Alzheimer's disease-like tau phosphorylation.* Biochem Biophys Res Commun, 2004. **319**(3): p. 993-1000.
73. Celniker, S.E. and G.M. Rubin, *The Drosophila melanogaster genome.* Annu Rev Genomics Hum Genet, 2003. **4**: p. 89-117.
74. Reiter, L.T., et al., *A systematic analysis of human disease-associated gene sequences in Drosophila melanogaster.* Genome Res, 2001. **11**(6): p. 1114-25.
75. Prussing, K., A. Voigt, and J.B. Schulz, *Drosophila melanogaster as a model organism for Alzheimer's disease.* Mol Neurodegener, 2013. **8**: p. 35.
76. Bonner, J.M. and G.L. Boulianne, *Drosophila as a model to study age-related neurodegenerative disorders: Alzheimer's disease.* Exp Gerontol, 2011. **46**(5): p. 335-9.
77. Fernandez-Moreno, M.A., et al., *Drosophila melanogaster as a model system to study mitochondrial biology.* Methods Mol Biol, 2007. **372**: p. 33-49.
78. Ong, C., et al., *Drosophila melanogaster as a model organism to study nanotoxicity.* Nanotoxicology, 2015. **9**(3): p. 396-403.
79. Brand, A.H. and N. Perrimon, *Targeted gene expression as a means of altering cell fates and generating dominant phenotypes.* Development, 1993. **118**(2): p. 401-15.
80. Busson, D. and A.M. Pret, *GAL4/UAS targeted gene expression for studying Drosophila Hedgehog signaling.* Methods Mol Biol, 2007. **397**: p. 161-201.
81. St Johnston, D., *The art and design of genetic screens: Drosophila melanogaster.* Nat Rev Genet, 2002. **3**(3): p. 176-88.
82. Wilschefski, S.C. and M.R. Baxter, *Inductively Coupled Plasma Mass Spectrometry: Introduction to Analytical Aspects.* Clin Biochem Rev, 2019. **40**(3): p. 115-133.
83. Bulska, E. and B. Wagner, *Quantitative aspects of inductively coupled plasma mass spectrometry.* Philos Trans A Math Phys Eng Sci, 2016. **374**(2079).
84. Howard, J.W., et al., *UHPLC for the separation of proteins and peptides.* Bioanalysis, 2012. **4**(24): p. 2971-88.
85. Carr, D., *The Handbook of Analysis and Purification of Peptides and Proteins by Reversed-Phase HPLC*. 3 ed. 2002: Grace Vydac Technical Support Group. 69.
86. Zuvela, P., et al., *Column Characterization and Selection Systems in Reversed-Phase High-Performance Liquid Chromatography.* Chem Rev, 2019. **119**(6): p. 3674-3729.
87. Satoh, S., et al., *Simultaneous determination of alpha-lipoic acid and its reduced form by high-performance liquid chromatography with fluorescence detection.* J Chromatogr B Analyt Technol Biomed Life Sci, 2007. **854**(1-2): p. 109-15.
88. Robert, A., et al., *Regulation of copper and iron homeostasis by metal chelators: a possible chemotherapy for Alzheimer's disease.* Acc Chem Res, 2015. **48**(5): p. 1332-9.
89. Petersen Shay, K., et al., *Is alpha-lipoic acid a scavenger of reactive oxygen species in vivo? Evidence for its initiation of stress signaling pathways that promote endogenous antioxidant capacity.* IUBMB Life, 2008. **60**(6): p. 362-7.

90. Hager, K., et al., *Alpha-lipoic acid as a new treatment option for Alzheimer's disease--a 48 months follow-up analysis.* J Neural Transm Suppl, 2007(72): p. 189-93.

Lisa
rektori 07.04.2020 käskkirjale nr 1-8/17

Lihtlitsents lõputöö reprodutseerimiseks ja lõputöö üldsusele kättesaadavaks tegemiseks[1]

Mina, Gertrud Henna Sildnik

1. Annan Tallinna Tehnikaülikoolile tasuta loa (lihtlitsentsi) enda loodud teose, α-lipoehappe toimemehhanism vase metabolismile rakukultuuri ja äädikakärbse mudelites, mille juhendajad on Sigrid Kirss ja Peep Palumaa

1.1 reprodutseerimiseks lõputöö säilitamise ja elektroonse avaldamise eesmärgil, sh Tallinna Tehnikaülikooli raamatukogu digikogusse lisamise eesmärgil kuni autoriõiguse kehtivuse tähtaja lõppemiseni;

1.2 üldsusele kättesaadavaks tegemiseks Tallinna Tehnikaülikooli veebikeskkonna kaudu, sealhulgas Tallinna Tehnikaülikooli raamatukogu digikogu kaudu kuni autoriõiguse kehtivuse tähtaja lõppemiseni.

2. Olen teadlik, et käesoleva lihtlitsentsi punktis 1 nimetatud õigused jäävad alles ka autorile.

3. Kinnitan, et lihtlitsentsi andmisega ei rikuta teiste isikute intellektuaalomandi ega isikuandmete kaitse seadusest ning muudest õigusaktidest tulenevaid õigusi.

26.05.2022

[1] *Lihtlitsents ei kehti juurdepääsupiirangu kehtivuse ajal vastavalt üliõpilase taotlusele lõputööle juurdepääsupiirangu kehtestamiseks, mis on allkirjastatud teaduskonna dekaani poolt, välja arvatud ülikooli õigus lõputööd reprodutseerida üksnes säilitamise eesmärgil. Kui lõputöö on loonud kaks või enam isikut oma ühise loomingulise tegevusega ning lõputöö kaas- või ühisautor(id) ei ole andnud lõputööd kaitsvale üliõpilasele kindlaksmääratud tähtajaks nõusolekut lõputöö reprodutseerimiseks ja avalikustamiseks vastavalt lihtlitsentsi punktidele 1.1. jq 1.2, siis lihtlitsents nimetatud tähtaja jooksul ei kehti.*